UCID - 16328

LAWRENCE LIVERMORE LABORATORY

University of California/Livermore, California

STRAIN HARDENING IN THE HEMP CODE

W. L. Bradley

July 25, 1973

Prepared for U. S. Atomic Energy Commission under contract no. W-7405-Eng-48

DISCLAIMER

THIS PAGE

WAS INTENTIONALLY

LEFT BLANK

CONTENTS

STRAIN HARDENING IN THE HEMP CODE

ABSTRACT

The Prandtl-Reuss equations used in the HEMP elastic-plastic computer program are satisfied exactly for elastic, perfectly plastic materials, and are less exact for materials that strain harden. This paper presents a new method of incorporating strain hardening into the flow law that is exact for linear strain hardening and very nearly exact for nonlinear strain hardening. A tensile test of a strain-hardening material is simulated using the present method and the previous method. The original approximate method has an accumulated error of less than 2% when compared to the present method. The present method agrees with exact calculations to within 0.05%.

INTRODUCTION

In recent years computer programs have been developed to simulate the elastic, elastic-plastic, and hydrodynamic behavior of metals and other materials.[1,2] Initially, these assumed elastic, perfectly plastic behavior. Subsequently, the strain-hardening characteristics of materials were incorporated into the simulation. This paper reports a refinement in the way of introducing this strain-hardening behavior into the calculations. A stress-strain curve for a 5083 aluminum alloy has been simulated using the previous and the presently reported computational schemes to measure the improvement in precision gained in using the new method.

STRAIN-HARDENING COMPUTATIONS

Previous Computational Schemes

The yield condition of von Mises describes the elastic limit. In the principal stress space, depicted in Fig. 1a, the yield condition can be written as

$$(\sigma_1 - \sigma_2)^2 + (\sigma_2 - \sigma_3)^2 + (\sigma_3 - \sigma_1)^2 = 2(Y_0)^2 \qquad (1)$$

where the σ_i are the principal stresses and Y_0 is the yield strength in a simple tension test.

Since the computational scheme in the computer program uses deviatoric stresses,* it is convenient to restate Eq. (1) in terms of deviatoric stresses, as

$$(s_1 - s_2)^2 + (s_2 - s_3)^2 + (s_3 - s_1)^2 = 2(Y_0)^2 \qquad (2)$$

*The deviatoric stress, $s_{ii} = \sigma_{ii} + P$, where P is the hydrostatic stress component, i.e., $P = 1/3\,(\sigma_1 + \sigma_2 + \sigma_3)$.

By definition, $s_1 + s_2 + s_3 = 0$, which allows Eq. (2) to be simplified into

$$s_1^2 + s_2^2 + s_3^2 = \frac{2}{3} Y_0^2. \tag{3}$$

If $s_1^2 + s_2^2 + s_3^2$ is less than $\frac{2}{3} Y_0^2$, the material is within the elastic limit and Hooke's law may be used to calculate the stress deviators. Assume that the (n + 1) strain increment used with Hooke's law takes one beyond the yield surface, as shown in Fig. 1b. One must then correct the assumption of elasticity; this strain increment was, in fact, composed of an elastic and a plastic component. The elastic component moves along the yield surface and the plastic component moves perpendicular to the yield surface. Thus, the calculated stress must be relaxed back to the yield surface.

The magnitude of this relaxation is given by $(2\mu\Delta\epsilon^P)$. This relaxation is accomplished most conveniently by multiplying each of the stress deviators (s_1, s_2, s_3) by a scalar

$$m = \sqrt{\frac{2}{3}}\ Y_0 \Big/ \sqrt{s_1^2 + s_2^2 + s_3^2}.$$

The projection of the radius vector of the point at (n + 1) is thus scaled so that the point lies on the yield surface. The observed incompressibility of the plastic state is implicit in the above procedure.

Prandtl[3] and Reuss,[4] extending the Levy-Mises[5,6] equations to allow a strain increment to have an elastic and plastic component, assumed that

$$d\epsilon_{ij}^P = s_{ij} d\lambda. \tag{4}$$

The physical significance of Eq. (4) is that the plastic strain increment is assumed to be proportional to the deviatoric stress component. The geometric significance of Eq. (4) with respect to Fig. 1a is that it requires the plastic strain increment to be perpendicular to the yield surface.

Under what circumstance does the scaling procedure previously described satisfy this condition? Prior to scaling, s_{ii}^{n+1} may be described by

$$s_{ii}^{n+1} = s_{ii}^n + 2\mu\Delta\epsilon_{ii}^{'T} \tag{5}$$

where

s_{ii}^n = deviatoric stress prior to straining

$\Delta\epsilon_{ii}^{'T}$ = total deviatoric strain (elastic-plastic) increment

μ = shear modulus.

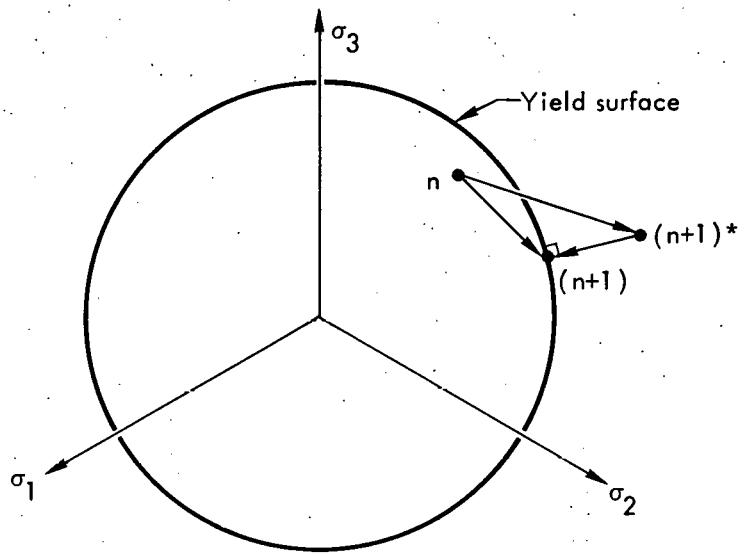

Fig. 1a. The von Mises yield assumption in $(\sigma_1, \sigma_2, \sigma_3)$ space.

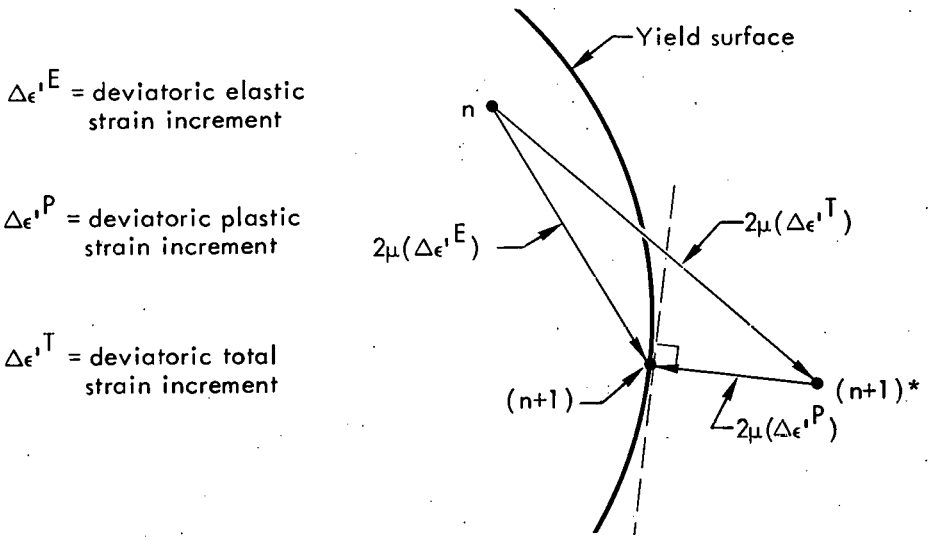

Fig. 1b. Schematic of the stress scaling procedure for elastic-plastic behavior. From n to $(n + 1)^*$ represents the stress calculation, assuming complete elasticity. From $(n + 1)^*$ to $(n + 1)$ represents the relaxation of the elastic stress to correct for the plastic part of the total strain. From n to $(n + 1)$ represents the actual increase in the elastic stress for the strain increment, $\Delta\epsilon'^T$.

After scaling, the deviatoric stress is given by

$$s_{ii}^{n+1} = m\left(s_{ii}^{n} + 2\mu\Delta\epsilon_{ii}^{'T}\right). \tag{6}$$

Furthermore, the incremental stress increase is given by

$$\Delta s_{ii}^{n+1/2} = m\left(s_{ii}^{n} + 2\mu\Delta\epsilon_{ii}^{'T}\right) - s_{ii}^{n}. \tag{7}$$

The plastic strain increment is the difference in the total deviatoric strain increment and the elastic deviatoric strain increment, or

$$\Delta\epsilon_{ii}^{P} = \Delta\epsilon_{ii}^{'T} - \frac{\Delta s_{ii}^{n+1/2}}{2\mu}. \tag{8}$$

Substituting (8) into (7) and rearranging terms, gives

$$\Delta\epsilon_{ii}^{P} = \Delta\epsilon^{'T}(1 - m) + \frac{s_{ii}^{n}}{2\mu}(1 - m). \tag{9}$$

But, according to the Prandtl-Reuss assumption,

$$\frac{\Delta\epsilon_{ii}^{P}}{s_{ii}} = d\lambda. \tag{10}$$

Substituting (9) into (10) and simplifying, gives

$$d\lambda = (1 - m)\left[\frac{\Delta\epsilon_{ii}^{'T}}{s_{ii}^{n}} + \frac{1}{2\mu}\right]. \tag{11}$$

If $d\lambda$ is to remain constant for i = 1, 2, 3, then

$$\frac{\Delta\epsilon_{11}^{'T}}{s_{11}^{n}} = \frac{\Delta\epsilon_{22}^{'T}}{s_{22}^{n}} = \frac{\Delta\epsilon_{33}^{'T}}{s_{33}^{n}}. \tag{12}$$

But Eq. (10) states that

$$\frac{\Delta\epsilon_{11}^{P}}{s_{11}^{n}} = \frac{\Delta\epsilon_{22}^{P}}{s_{22}^{n}} = \frac{\Delta\epsilon_{33}^{P}}{s_{33}^{n}}. \tag{13}$$

Thus, the scaling to the yield surface as described earlier satisfies the Prandtl-Reuss criterion exactly when the total deviatoric strain equals the plastic strain; i.e., there is no strain-hardening.

For a perfectly plastic material, the yield surface in $(\sigma_1, \sigma_2, \sigma_3)$ space may be pictured as a cylinder of axis [1i + 1j + 1k]. The scaling procedure moves one in a

direction perpendicular to the axis of the cylinder, and thus, perpendicular to the surface of the cylinder as required by the Prandtl-Reuss criteria. If strain hardening occurs, however, the yield surface in $[\sigma_1, \sigma_2, \sigma_3]$ space is more properly described by a truncated cone whose axis is also the [111] direction. Scaling (s_{11}, s_{22}, s_{33}) in this case again moves one in a direction perpendicular to the cone axis. This direction will not be perpendicular to the surface of the cone, however, and thus violates the Prandtl-Reuss criterion.

When strain hardening was added to the scaling scheme for (s_{11}, s_{22}, s_{33}) described above, the plastic strain in a given increment was used to calculate a new yield surface for the next increment. Thus the conic yield surface representing a material that strain hardens is approximated by a cylinder with an incrementally increasing diameter as shown in Fig. 2, or the effective-stress effective-plastic-strain curve is approximated by an incremental stress-strain curve as shown in Fig. 3.

The error introduced in such a scheme is a result of producing the plastic strain increment perpendicular to the incremental surfaces of the cylinder rather than to the truc conical yield surface. The error accrued in such a scheme should be negligible for small increments and moderate strain-hardening. Furthermore, the error approaches zero as the first derivativc of the stress-strain curve approaches zero.

New Computational Scheme

The present computational scheme requires at the outset a definition of the Prandtl-Reuss proportionality constant, $d\lambda$, as a function of the stress-strain behavior of the material to be simulated. Inverting the Prandtl-Reuss criterion of Eq. (4) gives

$$s_{ij} d\lambda = d\epsilon^P_{ij} . \tag{14}$$

Squaring each side of the equations given in tensor notation in (14) and adding the resulting equations gives

$$(s_{ij} s_{ij})(d\lambda)^2 = \left(d\epsilon^P_{ij}\, d\epsilon^P_{ij}\right) \tag{15}$$

where repeated indices are summed, i = 1, 2, 3.
Equation (15) may be rearranged to give

$$d\lambda = \frac{3}{2} \frac{\sqrt{2/3}\left(d\epsilon^P_{ij}\, d\epsilon^P_{ij}\right)^{1/2}}{\sqrt{3/2}(s_{ij} s_{ij})^{1/2}} = \frac{3}{2} \frac{d\bar{\epsilon}^P}{\bar{\sigma}} \tag{16}$$

where

$d\bar{\epsilon}^P$ = effective plastic strain

$\bar{\sigma}$ = effective stress.

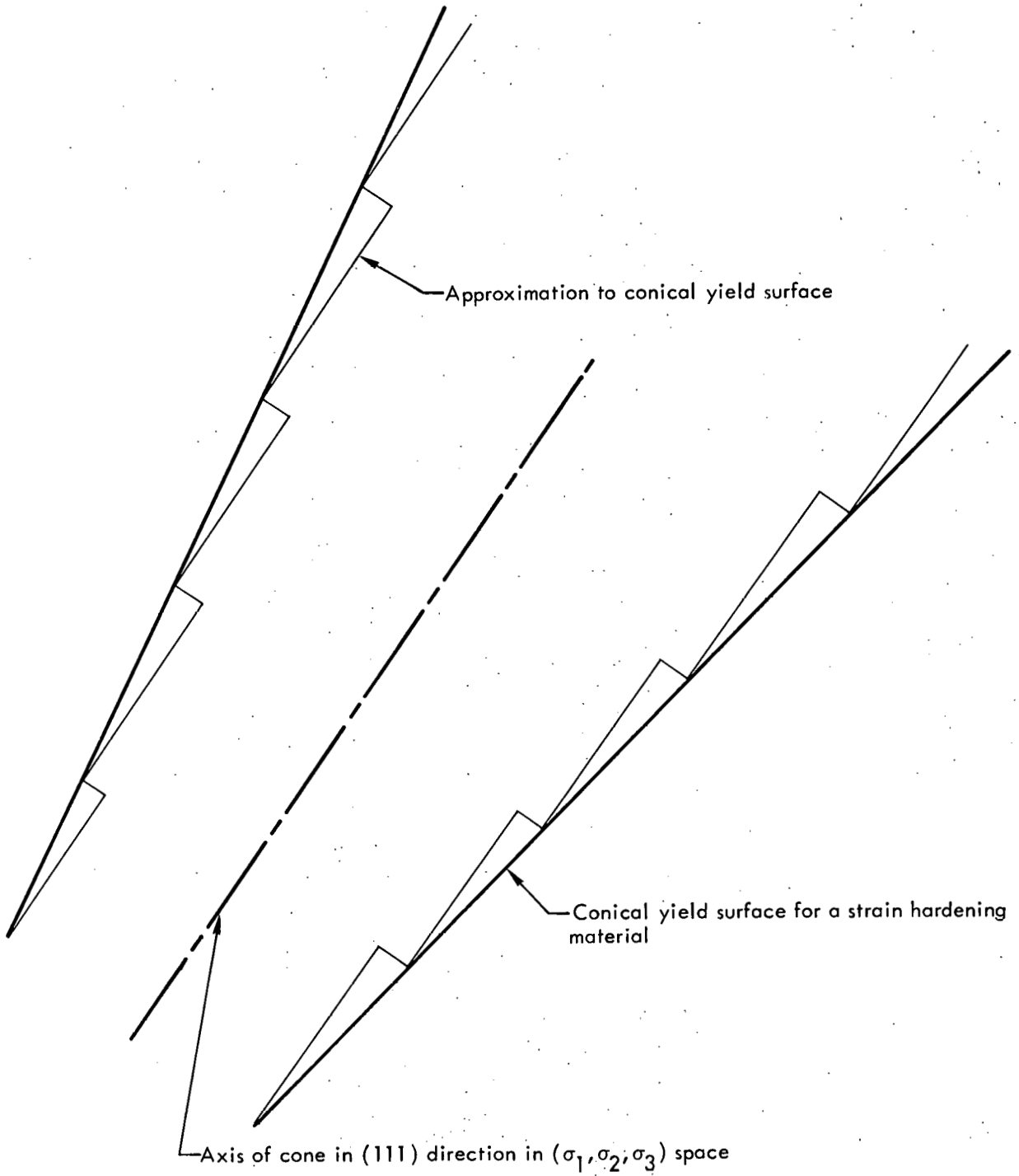

Fig. 2. True yield surface of a material that strain hardens ($\sigma = \sigma_0 + C\epsilon^P$) and the approximate yield surface used in the stress scaling computational scheme (pictured in $(\sigma_1, \sigma_2, \sigma_3)$ space).

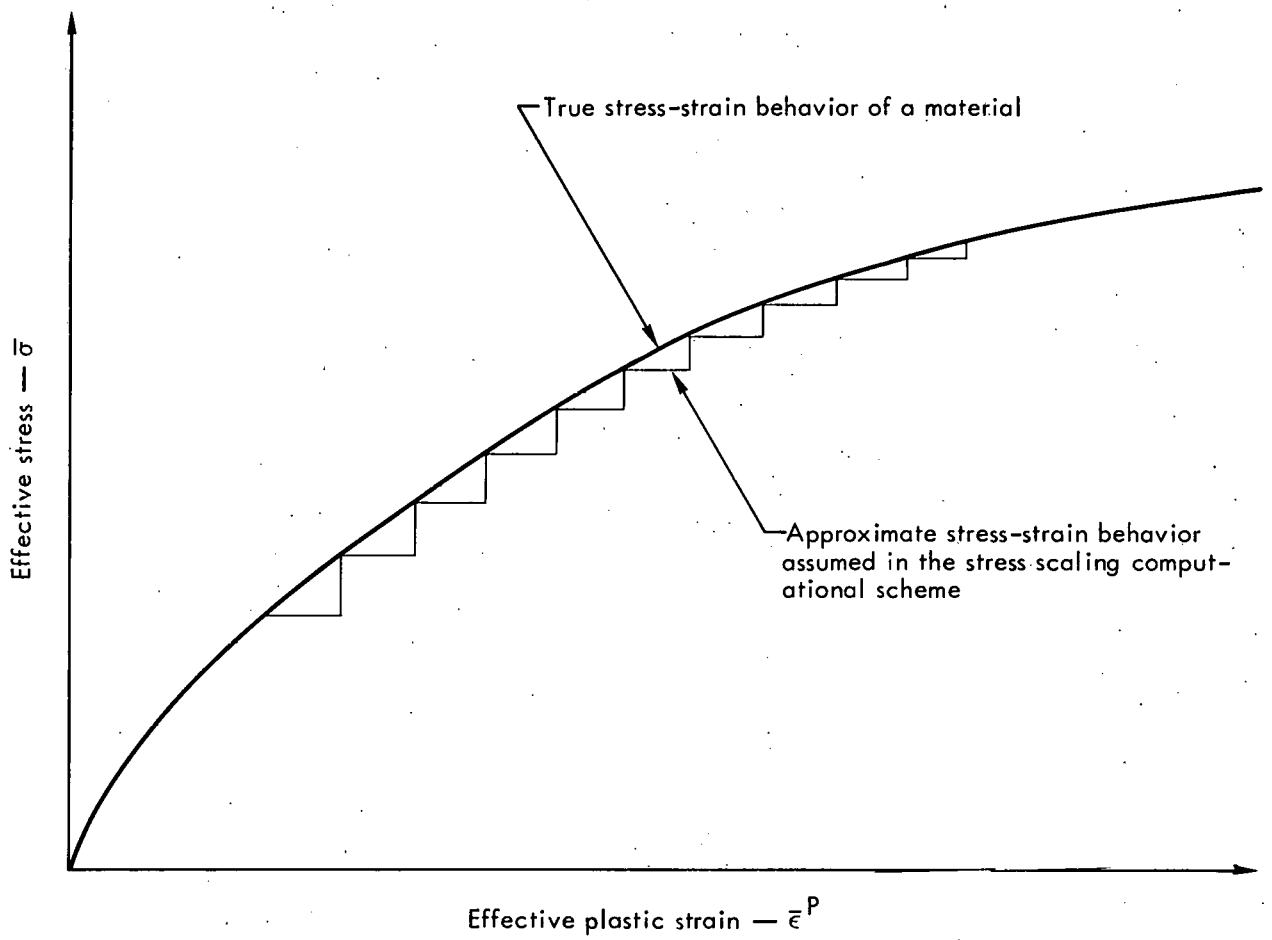

Fig. 3. A material's true stress-strain behavior and the approximate stress-strain behavior assumed in the stress scaling computational scheme.

The effective stress as a function of the effective plastic strain is most commonly determined in a tensile test. If the slope of the stress-strain curve at an effective plastic strain, $\bar{\epsilon}^P$, is given by $H' = \frac{d\bar{\sigma}}{d\bar{\epsilon}^P}$ then Eq. (16) may be rewritten as

$$d\lambda = \frac{3d\bar{\sigma}}{2\bar{\sigma}H'} . \tag{17}$$

Substituting (17) into (14) gives

$$d\epsilon_{ij}^P = \frac{3s_{ij}d\sigma}{2\bar{\sigma}H'} . \tag{18}$$

The incremental increase in the deviatoric stress can be calculated using Hooke's law, such that

$$ds_{ij} = 2\mu d\epsilon'^E_{ij} = 2\mu\left[d\epsilon'^T_{ij} - d\epsilon'^P_{ij}\right]. \tag{19}$$

Substituting (18) into (19) gives

$$ds_{ij} = 2\mu d\epsilon'^T_{ij} - \frac{3\mu s_{ij}}{\bar{\sigma}H'} d\bar{\sigma} . \tag{20}$$

Since

$$\bar{\sigma} = \sqrt{\frac{3}{2}} (s_{\ell m}s_{\ell m})^{1/2}$$

then

$$\bar{\sigma}^2 = \frac{3}{2} (s_{\ell m}s_{\ell m}) \tag{21}$$

and

$$2\sigma\, d\sigma = 3(s_{\ell m}ds_{\ell m}) \tag{22}$$

such that

$$d\bar{\sigma} = \frac{3}{2} \frac{s_{\ell m}}{\bar{\sigma}} ds_{\ell m} . \tag{23}$$

Substitution of (23) into (20) gives

$$ds_{ij} = 2\mu d\epsilon'^T_{ij} - \frac{9\mu s_{ij}(s_{\ell m}ds_{\ell m})}{2\bar{\sigma}H'} . \tag{24}$$

Equations (24) represent, in tensor notation for the most general case, six linear equations in six unknowns (ds_{ij}) for a given strain increment $d\epsilon'^T_{ij}$, stress state (s_{ij}) and strain-hardening materials characteristic (H'). In the Hydrodynamic-Elastic-Magneto-Plastic (HEMP) program,[1, 2] where this new strain-hardening calculation

was first utilized to simulate stress-strain curves for cylindrical tensile samples, $T_{23} = T_{13} = 0$. Therefore Eqs. (24 reduced to four equations in four unknowns. Since $s_{11} + s_{22} + s_{33} = 0$, $ds_{11} + ds_{22} + ds_{33} = 0$, and Eqs. (24) may be further reduced to three equations in three unknowns.

The solution of the simultaneous equations given in (24) partitions the total strain increment between elastic and plastic components in such a way that the stress increase produced by the plastic strain component equals exactly the stress increase predicted from the elastic stress component. The constant plastic volume condition is also satisfied implicitly in the formulation. Thus one begins the strain increment on the yield surface and also terminates the strain increment on the yield surface, eliminating further scaling back to the yield surface.

If the plastic portion of the effective-stress effective-strain curve is linear, the introduction of strain hardening into the formulation via Eqs. (24) is exact, the only error being that which is inherent in the finite difference approach. In terms of the yield surface, this requirement demands that the surface of the cone retain a constant angle of inclination with respect to its axis. If this angle changes or H' varies within a plastic strain increment, $\Delta\epsilon^P$, then we must approximate the average value of H' over the plastic strain increment in question, as in Fig. 4. This may be done to a first approximation by evaluating H' as follows:

$$H'^{n+1/2} = H'\left(\bar{\epsilon}^{P^n}\right) + H''\left(\bar{\epsilon}^{P^n}\right)\Delta\bar{\epsilon}^{P^{n-1/2}} . \qquad (25)$$

Since both $H''\left(\bar{\epsilon}^{P^n}\right)$ and $\Delta\bar{\epsilon}^{P^{n-1/2}}$ are quite small, it should normally be possible to neglect the second term in Eq. (25).

COMPARISON OF RESULTS, STRESS SCALING VS STRAIN-HARDENING SCHEMES

For a Single Iteration

Table 1 lists the data required to calculate $(ds_{ij})^{n+1/2}$ for the n^{th} cycle of a given computer simulation. Substituting these data into Eqs. (24)* produces the results listed in Table 2

From Eq. (4) the Prandtl-Reuss criterion is $\Delta\epsilon^P_{ij}/s_{ij} = d\lambda$. Comparing the figures in the last two columns of Table 2 shows the high precision with which this formulation maintains this criterion.

The same data given in Table 1 were then used again in the stress scaling calculation scheme. Here the strains are assumed to be completely elastic, and Hooke's law is used to calculate the stress increments and the new final stresses,

*A computational scheme that results from the simultaneous solution of Eqs. (24) appears in Appendix A.

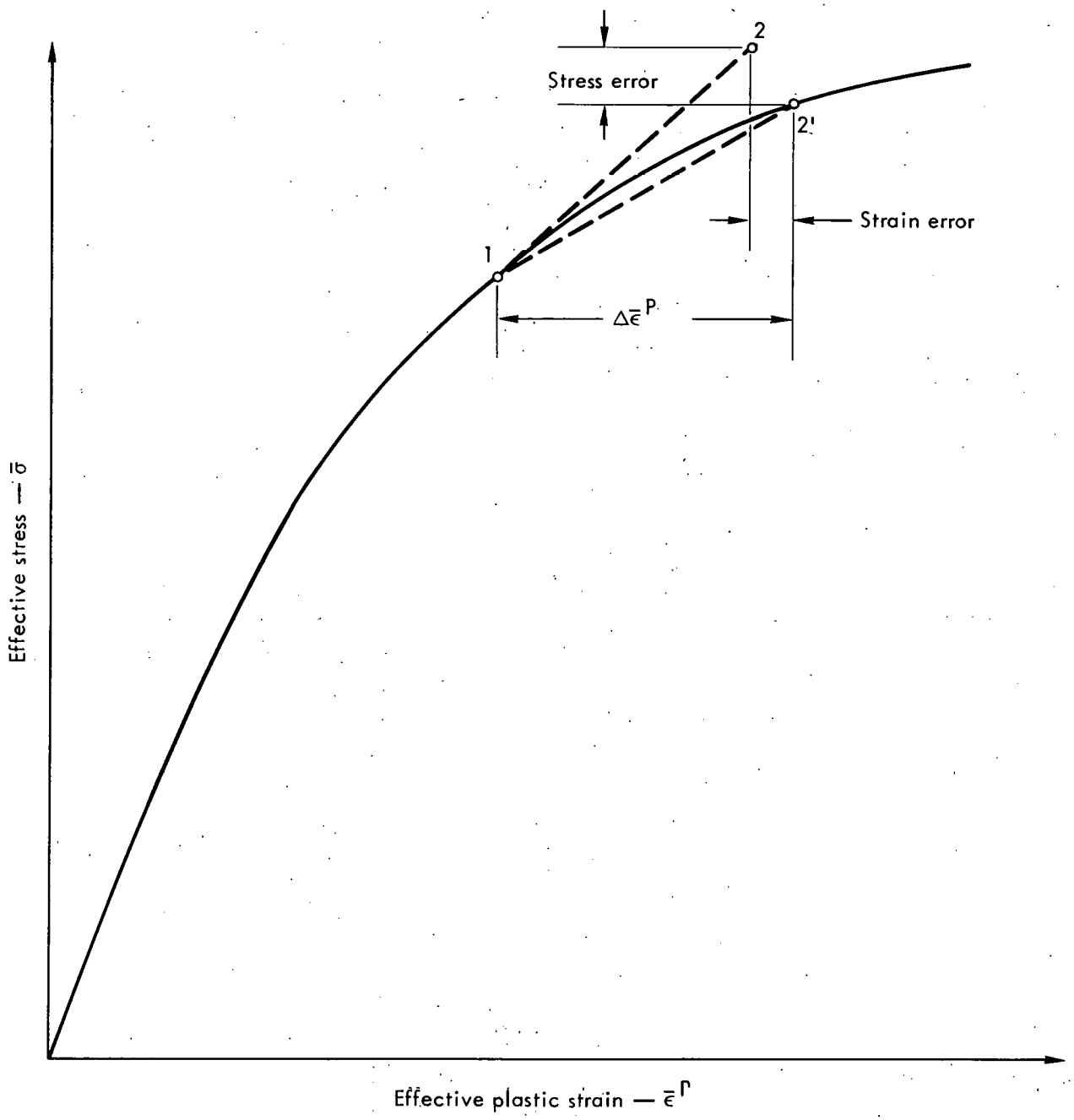

Fig. 4. Effective stress vs effective strain curve picturing the error that results from neglecting the variation of H' over the plastic strain interval $\Delta\epsilon^P$.

$s_{ij}^{n+1/2} = s_{ij}^{n} + \Delta s_{ij}^{n+1/2}$. Then the new stresses are scaled back to the yield surface, using the scalar $m = \sqrt{2/3}\, Y_0 / \sqrt{s_{ij} s_{ij}}$.

Normally the code calculates Y_0 for each cycle from the effective plastic strain total at the end of the previous cycle. These calculations, however, use the same Y_0 based on the data in Table 1, making the incremental stresses directly comparable with those of Table 2. Table 3 shows the results.

Table 1. Data for calculating $(s_{ij})^{n+1/2}$ for the n^{th} cycle of computer simulation.

ij	s_{ij} kbar	T_{ij} kbar	$\Delta\epsilon'^{T}_{ij}$ 10^{-6}
xx	1.6773	–	3.187226783
yy	-1.1128	–	-2.191054681
zz	-0.5645	–	0.9961721024
xy	–	1.6797	5.927840127
yz	–	0	0
xz	–	0	0

μ = 277 kbar H' = 4.0049 kbar

Table 2. Results of substituting the data of Table 1 into Eqs. (24).

ij	Δs_{ij} 10^{-3} kbar	ΔT_{ij} 10^{-3} kbar	$\Delta\epsilon^{P}_{ij}/s_{ij}$ 10^{-3} kbar^{-1}	$\Delta\epsilon^{P}_{ij}/T_{ij}$ 10^{-3} kbar^{-1}
xx	0.0752931589	–	1.819184733	–
yy	-0.0923329142	–	1.819184733	–
zz	0.0170397553	–	1.819184736	–
xy	–	-0.0508375539	–	1.819184734

Table 3. Results of parallel calculations to those of Table 2, starting with the data of Table 1 but this time using the stress scaling calculation scheme.

ij	Δs_{ij} 10^{-3} kbar	ΔT_{ij} 10^{-3} kbar	$\Delta\epsilon^{P}_{ij}/s_{ij}$ 10^{-3} kbar^{-1}	$\Delta\epsilon^{P}_{ij}/T_{ij}$ 10^{-3} kbar^{-1}
xx	0.073252	–	1.821381361	–
yy	-0.092757	–	1.818496831	–
zz	0.0167604	–	1.818291465	–
xy	–	0.0500070	–	1.818508727

The last two columns in Table 3 show that the Prandtl-Reuss criterion is satisfied fairly well, though not nearly as precisely as in the present formulation (Table 2). The generally good results displayed in Table 3 might be expected in view of the low value of H' used, corresponding to a point in the material's stress-strain behavior where very little strain hardening occurs. In areas where strain hardening takes place more rapidly the differences between Tables 2 and 3 would certainly be greater, as would the observed variation in $d\lambda$ in Table 3.

Complete Simulation of a Tensile Test

The HEMP code has been run with input boundary conditions and material constants set to simulate a tensile test on a 5083 aluminum alloy. The stress-strain behavior of material at the center of a cylinder has been simulated using the HEMP code with the strain scaling computational scheme and then rerun with the present strain-hardening scheme. The results are presented in tabular form in Table 4.

Table 4. Comparison of two different schemes for calculating stress and strain at the center of a cylinder for a test of 5083 aluminum alloy.

Lengthwise extension %	σ_{xx} Present scheme psi	σ_{xx} Scaling scheme psi	σ_{xx} Difference psi	ϵ_{xx} Present scheme 10^{-4}	ϵ_{xx} Scaling scheme 10^{-4}	ϵ_{xx} Difference 10^{-4}
2.5	38,205	38,323	118	214.7	218.3	3.6
5	42,356	42,437	81	457.0	459.4	2.4
7.5	45,546	45,594	48	697.7	698.6	0.9
10	48,166	48,187	21	935.7	934.9	-0.8
12.5	50,425	50,420	-5	1172.0	1169.0	-3.0
15	52,441	52,411	-30	1409	1404	-5
17.5	54,305	54,244	-61	1649	1640	-9
20	56,100	55,997	-103	1897	1883	-14
22.5	57,934	57,767	-167	2164	2141	-23
25	59,989	59,711	-278	2471	2432	-39

The strain simulated at the center of the cylindrical specimen using the two methods of incorporating strain hardening varies by as little as 0.00008 (0.01%) to as much as 0.0039 (1.6%). The stress variation between the two methods ranged from 5 psi (0.01%) to 278 psi (0.46%). Thus, the error accumulated in the stress scaling is shown to be only slight, at least in a tensile test of a 5083 aluminum alloy.

Internal Accuracy of Present Strain-Hardening Model

In the initial programming of the present strain-hardening scheme only the first term in Eq. (25) for H' is considered, the variation of H' over the strain interval, $\Delta\bar{\epsilon}^P$, in the stress-strain curve being neglected. The resulting error is pictured graphically in Fig. 4. Starting at (σ, ϵ) defined by point 1, the new strain-hardening method would iterate to (σ, ϵ) at point 2, rather than to point 2'. It can be seen that the resulting stress predicted is somewhat higher than the true value, while the resulting strain is somewhat lower than the actual value. In any given cycle, the stress calculated implicitly may be compared to a value calculated from the material characteristics and the plastic strain at that cycle. The difference in these two values estimates the error accumulated due to the variation of H' within a given $\Delta\bar{\epsilon}^P$.

This check was made in the simulation of the tensile test of a cylinder of 5083 aluminum alloy. The maximum variation between the calculated value and the correct value was 29.4 psi (0.05%), which was considered to be satisfactory.

SUMMARY

This new computational scheme partitions the total strain increment into elastic and plastic components, and makes the strain hardening associated with the plastic strain increment exactly equal the stress increase associated with the elastic increment

This procedure has been compared to an earlier, less exact method of incorporating strain hardening using stress scaling. For 1 cycle and for a whole simulation of over 15,000 cycles the stress scaling method error for this quasistatic tensile test was less than 2%.

Neglecting the variation in H' within the increments $\Delta\epsilon^P$ causes less than 0.05% error in the new strain-hardening calculation.

REFERENCES

1. M. L. Wilkins, "Calculation of Elastic-Plastic Flow," in Methods in Computational Physics (Academic Press, New York, 1964), vol 3, p. 211.
2. M. L. Wilkins, Calculation of Elastic Plastic Flow, Lawrence Livermore Laboratory, Rept. UCRL-7322, Rev. 1 (1969).
3. L. Prandtl, Proc. Int. Cong. App. Mech. 1st, Delft (1924), p. 43.
4. A. Reuss, Z. Angew. Math. Mech. 10, 266 (1930).
5. M. Levy, Compt. Rend. 70, 1323 (1870).
6. R. von Mises, Z. Angew. Math. Mech. 8, 161 (1928).

APPENDIX A

$$C_1^{n+1} = \frac{2(\bar{\sigma}^n)^2 H'^n}{9\mu} \tag{A1}$$

$$C_2^{n+1} = 2\mu\, C_1^{n+1} \tag{A2}$$

$$C_3^{n+1} = \frac{2T_{xy}^n}{\frac{C_1}{T_{xy}^n}^n + 2T_{xy}} \tag{A3}$$

$$C_4^{n+1} = \frac{\frac{C_1}{s_x^n}}{\left(C_3 - 1\right)\left(s_x^n - s_z^n\right) - \frac{C_1}{s_x^n}} . \tag{A4}$$

$$\Delta s_y^{n+1/2} = \frac{C_2\left[C_4\left(\frac{C_3\Delta\epsilon'^{\,n+1/2}_{xy}}{2T_{xy}^n} - \frac{\Delta\epsilon'^{\,n+1/2}_{x}}{s_x^n}\right) + \frac{\Delta\epsilon'^{\,n+1/2}_{y}}{s_y^n} - \frac{\Delta\epsilon'^{\,n+1/2}_{x}}{s_x^n}\right]}{\left[\left(C_3 - 1\right)\left(s_y^n - s_z^n\right) C_4 + \frac{C_1}{s_y^n}\right]} \tag{A5}$$

$$\Delta s_x^{n+1/2} = \frac{C_2\left(\frac{\Delta\epsilon'^{\,n+1/2}_{x}}{s_x^n} - \frac{\Delta\epsilon'^{\,n+1/2}_{y}}{s_x^n}\right) + \Delta s_y^{n+1/2}\left(\frac{C_1}{s_y^n}\right)}{\left(\frac{C_1}{s_x^n}\right)} \tag{A6}$$

$$\Delta T_{xy}^{n+1/2} = \frac{\frac{C_2}{s_y^n}\Delta\epsilon'^{\,n+1/2}_{y} - \Delta s_x^{n+1/2}\left(s_x^n - s_z^n\right) - \Delta s_y^{n+1/2}\left(\frac{C_1}{s_y^n} + s_y^n - s_z^n\right)}{2T_{xy}^n} \tag{A7}$$

$$s_x^{n+1} = s_x^n + \Delta s_x^{n+1/2} \tag{A8}$$

$$s_y^{n+1} = s_y^n + \Delta s_y^{n+1/2} \tag{A9}$$

$$s_z^{n+1} = -\left(s_x^{n+1} + s_y^{n+1}\right) \tag{A10}$$

$$T_{xy}^{n+1} = T_{xy}^n + \Delta T_{xy}^{n+1/2} \tag{A11}$$

DISTRIBUTION

LLL Internal Distribution

G. A. Broadman
R. B. Carr
S. Fernbach
E. D. Giroux
C. R. Henry
J. S. Kahn
V. N. Karpenko
V. Kransky
W. A. Lokke
T. Perlman
R. J. Wasley
P. Weidhaas
M. L. Wilkins 5
TID File 30

External Distribution

J. Mescall
Army Materials & Mechanics Research Center
Watertown, Massachusetts

P. J. Blewett
Los Alamos Scientific Laboratory
Los Alamos, New Mexico

F. A. McClintock
Massachusetts Institute of Technology
Cambridge, Massachusetts

L. D. Bertholf
Sandia Laboratories
Livermore California

R. Haufman
Physics International
San Leandro, California

G. E. Duvall
Washington State University
Pullman, Washington

W. L. Bradley 5
Colorado School of Mines
Golden, Colorado

RBC:edas

External Distribution (Continued)

Technical Information Center, Oak Ridge 2

RBC:eds:lm